

# Hydrothermal synthesis of TiO<sub>2</sub> anatase nanocrystals using hexaprismatic-shaped oxo-carboxylate complexes

Adel Rammal, Frédéric Brisach, Marc Henry\*

Laboratoire de chimie moléculaire de l'état solide, université Louis-Pasteur, Institut Le-Bel, 4, rue Blaise-Pascal, 67070 Strasbourg cedex, France

Received 12 June 2001; accepted 16 July 2001

**Abstract** – The molecular structural chemistry of titanium oxo-carboxylate complexes is critically reviewed with particular emphasis on the understanding of the various characterised molecular shapes. Among the four crucial parameters thought to have a structural influence on these shapes (nature of the OR alkoxy group, molar ratio  $C = O/Ti$ , stoichiometric ratio  $S = XCOOH/Ti$  and chemical nature of the carboxylic X moiety), it was concluded that the nature of R group, the C ratio and the steric hindrance of X were of minor importance. From the available data, it was also concluded that a high S ratio seems to favour corner-sharing versus edge-sharing of TiO<sub>6</sub> octahedra and that it was not possible to establish a clear correlation between the pK<sub>a</sub> value of the carboxylic acid and the observed molecular shape. During this study, a new titanium oxo-carboxylate complex was obtained by reacting titanium isopropoxide with phenylacetic acid (PAAH, X = PhCH<sub>2</sub> at S = 3/2). This hexaprismatic Ti<sub>6</sub>O<sub>6</sub>(OPr<sup>i</sup>)<sub>6</sub>(PAA)<sub>6</sub> complex was characterised by single-crystal X-ray diffraction and used as a molecular precursor of TiO<sub>2</sub> anatase nanocrystals after hydrolysis by NMe<sub>4</sub>OH and autoclaving at T = 200 °C. The size and size distribution of these nanocrystals were found to decrease as the R = Ti/NMe<sub>4</sub> ratio was increased. Nucleation and growth of anatase nanocrystals was found to be deeply modified by the presence of phenylacetate ions in the solution, but there was no evidence of an influence of the molecular anisotropy of the molecular precursor on the final shape of the nanocrystals. **To cite this article:** A. Rammal et al., C. R. Chimie 5 (2002) 59–66 © 2002 Académie des sciences / Éditions scientifiques et médicales Elsevier SAS

hydrothermal synthesis / titanium oxo-carboxylates / nanocrystals / titania / anatase

**Résumé** – Les structures moléculaires des oxo-carboxylates de titane connus à ce jour ont été passées en revue de manière critique. Parmi les quatre paramètres cruciaux pouvant avoir une influence sur la forme moléculaire (nature du groupement alkyle R, rapport molaire  $C = O/Ti$ , rapport stœchiométrique  $S = XCOOH/Ti$  et nature du radical X), on constate que la nature de R, le rapport C et l'encombrement stérique procuré par le radical X n'ont qu'une importance mineure. À partir des données collectées, on peut aussi conclure qu'un rapport S élevé favorise, pour les octaèdres TiO<sub>6</sub>, le partage des sommets au détriment du partage d'arêtes. Par ailleurs, il n'a pas été possible d'établir une relation claire entre le pK<sub>a</sub> de l'acide carboxylique utilisé et la structure moléculaire finale des complexes. Au cours de cette étude, un nouvel oxo-carboxylate de titane a été obtenu en faisant réagir l'isopropoxyde de titane avec l'acide phénylacétique (PAAH, X = PhCH<sub>2</sub>) dans un rapport S = 3/2. Par diffraction des rayons X sur monocristal, il a été montré que ce nouveau complexe, de formule Ti<sub>6</sub>O<sub>6</sub>(OPr<sup>i</sup>)<sub>6</sub>(PAA)<sub>6</sub>, adoptait une forme prismatique hexagonale déjà connue. Ces complexes ont été ensuite hydrolysés par l'hydroxyde de tétraméthylammonium en solution aqueuse et autoclavés à T = 200 °C pendant une nuit, afin de les transformer en nanocristaux d'anatase. On constate que la taille des cristaux diminue et que la distribution de taille des cristaux se rétrécit lorsque le rapport R = Ti/NMe<sub>4</sub> augmente. La nucléation et la croissance de ces nanocristaux d'anatase semble être de plus profondément affectée par la présence des ions phénylacétate dans la solution. Toutefois, aucune corrélation n'a pu être établie entre la forte anisotropie moléculaire des précurseurs de départ et la forme finale des nanocristaux. **Pour citer cet article :** A. Rammal et al., C. R. Chimie 5 (2002) 59–66 © 2002 Académie des sciences / Éditions scientifiques et médicales Elsevier SAS

synthèse hydrothermale / oxo-carboxylates de titane / nanocristaux / oxyde de titane / anatase

\* Corresponding author.

E-mail address: henry@chimie.u-strasbg.fr (M. Henry).

## 1. Introduction

The rational synthesis and study of nanocrystalline materials appears to be a new challenge in materials chemistry. Owing to their demonstrated technological importance (photoluminescence, solar energy conversion, photocatalysis, etc.), nanoarchitected semiconductor particles are very promising for designing new solid-state devices. For this purpose, and despite its rather wide band gap (3.2 eV),  $\text{TiO}_2$  is an attractive material as it is cheap, non-toxic and highly insoluble in water. These properties allow  $\text{TiO}_2$ -based nanoparticles to be used in a wide range of processes with minimal environmental impact [1]. Among the numerous methods that can be used to produce  $\text{TiO}_2$  nanocrystallites (see [1] and references herein), we have selected the hydrothermal technique as it is well suited for obtaining crystalline compounds and could lead to low-temperature phases or metastable structures [2]. Our starting point was a paper showing that it was possible to obtain quite monodisperse anatase nanocrystals (about 20 nm in length) after hydrolysis and polycondensation of titanium alkoxides  $\text{Ti}(\text{OR})_4$  in the presence of tetramethylammonium hydroxide  $\text{Me}_4\text{NOH}$  [3]. Here we report some preliminary results obtained by using titanium oxo-carboxylates instead of titanium alkoxides. Our aim was to see if by changing the molecular structure of the starting titanium complex, we would be able to detect a change in structure, size or shape of these nanocrystals. Carboxylic compounds were selected for this study as they are known to bond strongly with titanium atoms [4–15] and thus would be expected to remain strongly adsorbed during crystal growth in solution. From a molecular standpoint this study was also devoted to the synthesis and characterisation of new oxo-carboxylate compounds in order to get a deeper understanding of the crystal chemistry of these complexes, which are widely used in sol-gel chemistry [16] or in supramolecular metallo-organic chemistry [17].

## 2. Results and discussion

### 2.1. Molecular compounds

Fig. 1 gives a graphical overview of the current knowledge of the crystal chemistry of these titanium oxo-carboxylates. A first striking feature is that in all investigated compounds, titanium atoms are found in six-fold coordination. This is in big contrast with other titanium (oxo)alkoxides displaying four-fold [18], five-fold [18–20] and even seven-fold [20] coordinated titanium atoms. Concerning the various observed molecular shapes, we find, using the  $\text{TiO}_6$

octahedron as a primary building-unit, edge-sharing (bicyclane a) or corner-sharing (oxolane b) isolated dimers. Further edge sharing at right angle between two dimers leads to the cubane ( $2 \times a = e$ ) or the butterflyane ( $a + b = d$ ) shapes. Corner sharing between monomers and/or bicyclane dimers leads to the rutilane (h), the octacyclane (j) or the nonacyclane (k) shapes. Edge sharing between a monomer and the oxolane shape (b) leads to the important tricyclane secondary building-unit (c). Further association of these trimers through edge sharing leads to the anatasane (f) or hexaprismane shapes (i) respectively. Finally, association of two trimers through corner sharing leads to the bitricyclane shape (g). Obviously, these considerations are just a convenient way of rationalising experimental facts and should not be confused with the real mechanisms of condensation, which still remain quite obscure. As carboxylic ligands are nowadays extensively used for the rational design of supramolecular compounds [17], it seems of the utmost importance to identify the key factors that control the molecular shapes identified in this family of compounds. A detailed analysis of the situation shows that at least four main factors may be invoked.

(i) The chemical nature of the OR group of the starting  $\text{Ti}(\text{OR})_4$  alkoxide (R-effect). The minor importance of the R-effect is demonstrated by the isolation of the rutilane shape for  $\text{R} = \text{Et}, \text{Pr}^i, \text{Bu}^n$ ; of the cubane shape with  $\text{R} = \text{Et}, \text{Pr}^i, \text{Bu}^n, \text{Ph}$  and of the hexaprismane shape with  $\text{R} = \text{Et}$  or  $\text{Pr}^i$ .

(ii) The condensation molar ratio  $C = \text{O}/\text{Ti}$ . As shown in Fig. 1, different shapes may be obtained for the same  $C$  value: oxolane or butterflyane shapes for  $C = 0.5$ , anatasane, rutilane or bitricyclane for  $C = 2/3$  and cubane versus hexaprismane shapes for  $C = 1$ . Consequently, it cannot be said that the O/Ti ratio governs the molecular shape. At this stage, one may also discriminate between two different pathways: hydrolytic (ROH elimination) versus thermolytic ( $\text{R}_2\text{O}$  and/or  $\text{R}'\text{CO}_2\text{R}$  elimination) condensations. The fact that water was not necessary for obtaining the bitricyclane shape was nicely demonstrated by the use of methylidyne-carboxylic–nonacarbonyl–tricolbalt acid [11]. This observation obviously raises considerable doubts about the real occurrence of the hydrolytic pathway in solution. As all crystals are obtained after ageing of a mother liquor and as ageing or heating is known to promote oxolation through  $\text{R}_2\text{O}$  or  $\text{R}'\text{CO}_2\text{R}$  elimination [11,14], there is no need to invoke the esterification reaction to justify the formation of oxo-complexes. Further work is thus needed to clarify this point.

(iii) The stoichiometric ratio  $S = \text{XCOOH}/\text{Ti}$ . The transformation bitricyclane  $\rightarrow$  rutilane was observed for  $C = 0.67$  and  $\text{X} = \text{CH}_3$  by increasing this ratio

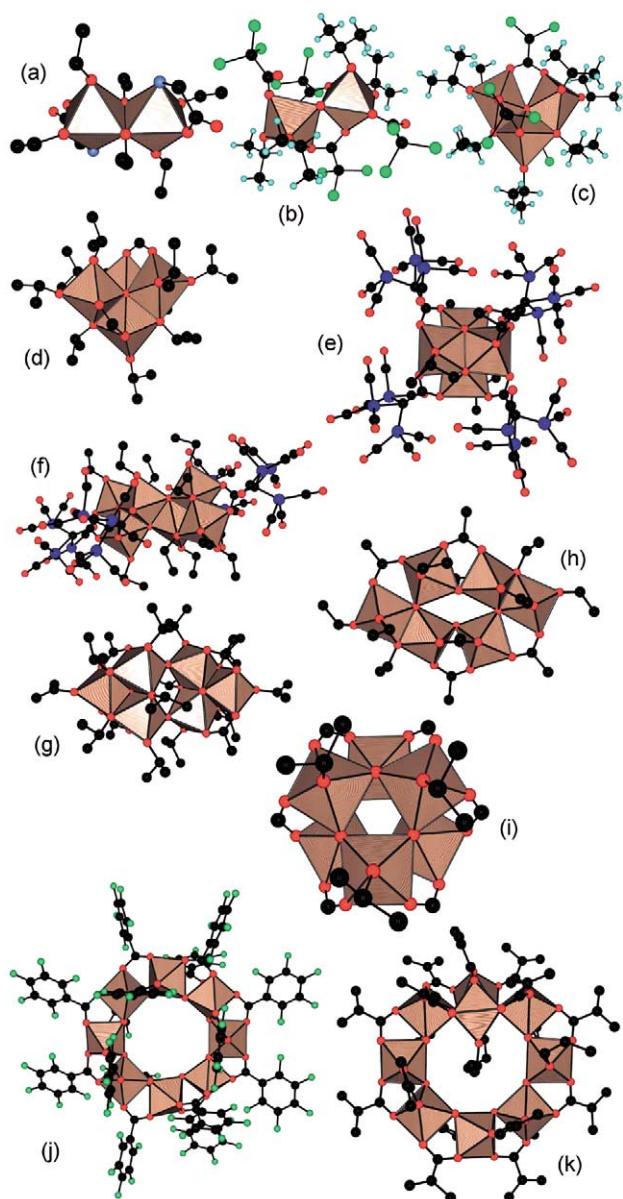


Fig. 1. Molecular structures, symbolic shapes and condensation ratios  $C = O/Ti$  for currently known titanium oxo-carboxylate compounds. **a.**  $Ti_2(OEt)_6(H_2NCH_2COO)_2$  [8] (bicyclane shape,  $C = 0$ ). **b.**  $Ti_2(OPr^i)_2(HOPr^i)_2(O_2CCCl_3)_4$  [15] (oxolane shape,  $C = 0.5$ ). **c.**  $Ti_3O(OPr^i)_7(O_2CCCl_3)_3$  [15] (tricyclane shape,  $C = 0.33$ ). **d.**  $Ti_4O_2(OPr^i)_{10}(HCOO)_2$  [12] (butterflane shape,  $C = 0.5$ ). **e.**  $Ti_4O_4(OR)_4(CoAc)_4$ ,  $R = Et, Pr^i, Bu^i, Ph$ ;  $CoAc = [(CO)_3Co]_3C-COO$  [10,11] (cubane shape,  $C = 1$ ). **f.**  $Ti_6O_4(OR)_{12}(COOR')_4$ ,  $R = Et, R' = CoAc$  [10];  $R = Pr^i, R' = CH_2CMe_3$  [12] (anatatasane shape,  $C = 0.67$ ). **g.**  $Ti_6O_4(OPr^i)_{12}(OAc)_4$  [6] (bitricyclane shape,  $C = 0.67$ ). **h.**  $Ti_6O_4(OR)_8(O_2CCH_3)_8$ ,  $R = Et$  [4],  $Pr^i$  [7],  $Bu^i$  [5] (rutilane shape,  $C = 0.67$ ). **i.**  $Ti_6O_8(OR)_6(O_2CR')_6$ ,  $R = Pr^i, R' = H$  [12];  $R = Et, Pr^i, R' = Me, PhOC_6H_4$  [14];  $R = Pr^i, R' = CHCl_2$  [15]; (hexaprismane shape,  $C = 1$ ). **j.**  $Ti_8O_8(O_2CC_6F_5)_8$  [9] (octacyclane shape,  $C = 1$ ). **k.**  $Ti_9O_8(OPr^i)_4(OMc)_{16}$ ,  $Mc = CH_2C(Me)CO$  [13]; (nonacyclane shape,  $C = 0.89$ ).

from 1 to 2. Similarly, tricyclane ( $S = 1, C = 1/3$ )  $\rightarrow$  oxolane ( $S = 2, C = 1/2$ ) or butterflane ( $S = 1,$

$C = 1/2$ )  $\rightarrow$  hexaprismane ( $S = 2, C = 1$ ) transformations were evidenced with  $X = CCl_3$  or  $X = H$  respectively. However, in these cases the  $C$  ratios were not constant as in the previous case. On the other hand with  $X = C[Co(CO)_3]_3$  no effect was observed [11]. In the same spirit, the hexaprismane shape can be obtained either at  $S = 1$  with  $X = CHCl_2$  or at  $S = 2$  with  $X = CH_3$  or  $PhOC_6H_4$ . Finally, it is interesting to note that octacyclane ( $S = 3$ ) and nonacyclane ( $S = 4$ ) shapes were obtained using acids in excess ( $S > 2$ ). Based on the currently available crystal structures, it then seems clear that a high  $S$  ratio promotes corner sharing over edge sharing for  $TiO_6$  octahedra. However, as before, much experimental work remains to be done before drawing a definitive conclusion.

(iv) The substituting moiety  $X$  of the carboxylic acid  $XCOOH$  used. Under this heading, two different aspects should be considered: the molecular geometry (steric effect) and the  $pK_a$  value (electronic effect) of the carboxylic acid used. Concerning the ligand's bulkiness, one may notice that the same hexaprismane shape is obtained with  $X = H, CH_3, PhOC_6H_4$  or  $CCl_3$ , meaning that shape selectivity should not be associated with steric hindrance for these systems. Consequently, as already suggested [12], acidity of the ligand (electronic effects) is expected to be a major factor governing structural changes. As shown in the Table 1, the cubane shape was uniquely obtained with the least acid compound  $X = C[Co(CO)_3]_3$ , while the most acid ones ( $X = H, PhOC_6H_4$  or  $CCl_3$ ) seem to prefer the hexaprismane shape. A compound having the same stoichiometry  $[Ti_6O_6(OPr^i)_6(O_2CCH_3)_6]$  was obtained by refluxing a 1:2 solution of  $Ti(OPr^i)_4$  and acetic acid in toluene, but its detailed molecular structure remains unknown as it was only characterised using IR and  $^1H$  NMR spectroscopy [14] and not by X-ray diffraction. To check this point a little bit further, we have investigated the reaction between phenylacetic acid  $PhCH_2COOH$  (PAA) and titanium isopropoxide  $Ti(OPr^i)_4$ . This ligand was selected because it is similar to acetic acid through its  $pK_a$  value (table 1 I), but shares with  $PhOC_6H_4COOH$  a common feature (occurrence of phenyl groups). It was also interesting with respect to the fact that it was apparently impossible to obtain single crystals with the closely related molecule  $C_6F_5CH_2COOH$  [9]. As we succeeded to get single-crystals at  $S = 3/2$ , we had the opportunity to increase this very interesting little family by one member. As shown in Fig. 2, the compound obtained may be formulated as  $[Ti_6(\mu_3-O)_6(C_6H_5CH_2COO)_6(OPr^i)_6]$  and displays the hexaprismane shape. As in similar compounds [12,14,15], the core of this molecule is made of two superposed  $Ti_3O_3$  hexagons ( $\langle d_{Ti-O} \rangle = 190.2$  pm) in eclipsed conformation. These hexagons are not regular with

Table 1. Effect of substitution on  $pK_a$  values of carboxylic acids R-COOH. All values from [21], except for  $(CO)_9Co_3(\mu_3-C)COOH$  [22].

R	$[(CO)_3Co]_3C$	$CH_3$	$PhCH_2$	$CH_2=C(Me)$	H	$C_6H_4OPh$	$H_2NCH_2$	$CCl_3$
$pK_a$	~6.4	4.76	4.31	4.25	3.75	3.53	2.35	0.66

Ti–O–Ti and O–Ti–O bond angles equal on average to  $134.8^\circ$  and  $101.9^\circ$  respectively. These two hexagons are further linked through oxo bridges ( $d_{Ti-O} = 217.8$  pm) with bond angles  $100.3^\circ$  (Ti–O–Ti) and  $77.7^\circ$  (O–Ti–O). Around this hexagonal  $Ti_6O_6$  prism, six PAA ligands bridging two titanium atoms (one above and one below) are found with their benzene rings capping each  $Ti_2O_2$  rectangular face. The coordination mode of the carboxylic group is found to be completely symmetric with  $d_{Ti-O} = 206.9$  pm and with a bite angle of  $124.6^\circ$ . These values are very similar to that found with the acetic acid ligand. As in the crystal structure of  $Ti_6O_6(OPr^i)_6(O_2CCl_3)_6$  [15], these prismatic hexamers are further associated into chains through van der Waals interactions between isopropoxy and PAA ligands (Fig. 2b). This is big contrast with the crystal structure of  $Ti_6O_6(OPr^i)_6(O_2CH)_6$ , where van der Waals dimers are formed through isopropoxy groups (Fig. 2c). Van der Waals chains also occur in  $Ti_6O_6(OPr^i)_6(O_2C_6H_4OPh)_6$ , but here they appear to be solvated by toluene molecules [14].

The occurrence of this hexaprismane core with a carboxylic acid more sterically hindered but displaying a  $pK_a$  value very similar to that of acetic acid fills a gap between acetic acid and phenoxybenzoic acid. It also shows that considerable work remains to be done in order to be able to predict the final molecular shape from the knowledge of the geometries of the starting compounds.

## 2.2. Nanocrystals

In order to detect any influence of the starting molecular shape of the metallo-organic oxo-carboxylate precursor on the final structure, shape and size of the  $TiO_2$  nanocrystals, we have selected the hexaprismane geometry. One of the obvious reason for this choice is that it is readily obtained by reacting phenylacetic acid with titanium isopropoxide. The other reason is that this shape provides a very special and interesting tubular disposition of the remaining isopropoxy groups. As carboxylate groups appear to be much less sensitive towards hydrolysis than OR groups [16], one may wonder if this molecular anisotropy could influence the morphology of the final crystalline oxide. In a first experiment, we have tried to reproduce the results of reference [3] where titanium isopropoxide has been hydrolysed by  $Me_4NOH$  at a ratio  $R = Ti/Me_4N^+ = 3$ , leading to sols of triangular

prismatic anatase nanocrystals (10–20 nm in size). Despite several trials, we have been unable to reproduce these results. Under TEM our sols appear to be amorphous with no particular noticeable size or shape. As autoclaving these sols at 175 and 200 °C was reported to lead to rectangular nanocrystals about  $28 \pm 3$  nm in length and  $12 \pm 2$  nm in width [3], a similar treatment was applied to our sols. Fig. 3 shows that our amorphous sols are indeed transformed into anatase nanocrystals about  $L = 22(7)$  nm in length and  $W = 13(3)$  nm in width. Besides a rather non-uniform size distribution, at least three different shapes are coexisting (globular, rectangular and triangular). This lack of reproducibility was attributed to the highly hygroscopic nature of titanium isopro

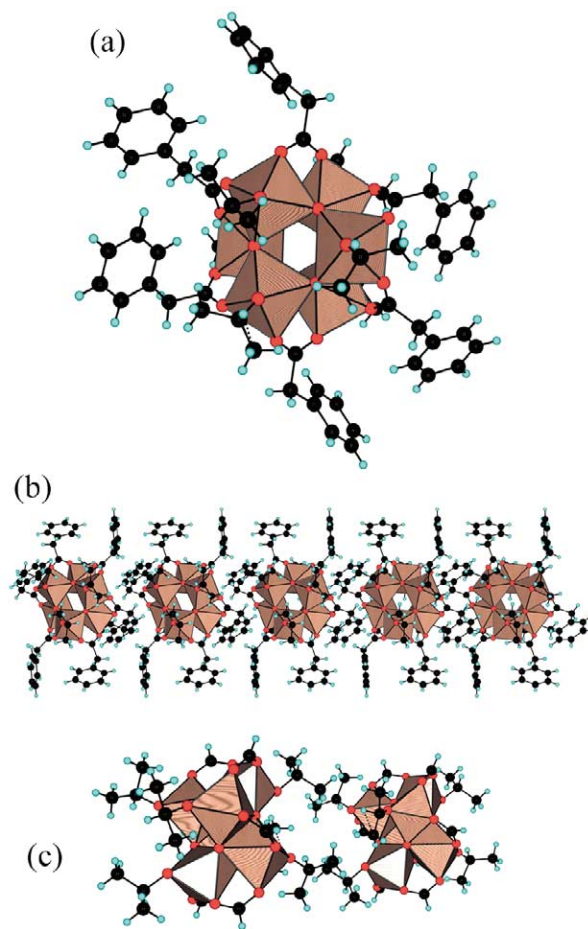


Fig. 2. a. Hexagonal prismatic molecular structure of  $Ti_6O_6(OPr^i)_6(C_6H_5CH_2COO)_6$ . b. van der Waals chain of hexagonal prisms in the solid state. c. van der Waals dimer of hexagonal prisms in the crystal structure of  $Ti_6O_6(OPr^i)_6(HCOO)_6$  [12].

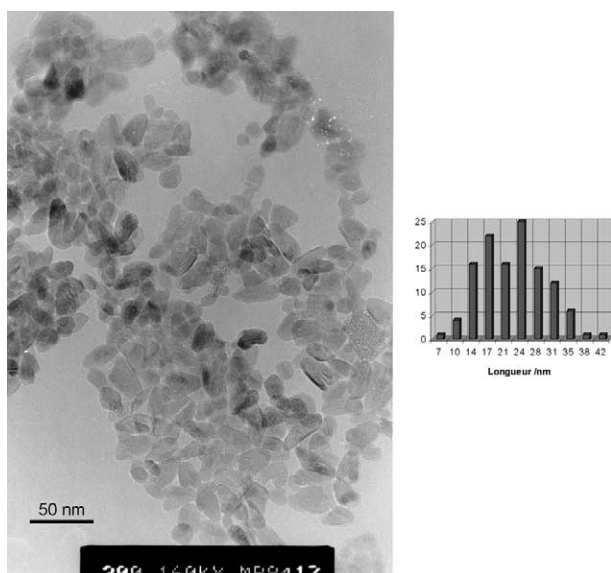


Fig. 3. TEM micrograph and size distribution of anatase nanocrystals obtained after hydrolysis and autoclaving ( $T = 200\text{ }^{\circ}\text{C}$ ) of  $\text{Ti}(\text{O-Pr}^i)_4$  solutions at  $R = \text{Ti}/\text{NMe}_4^+ = 3$ . Average sizes and standard deviations are  $22(7) \times 13(3)$  nm.

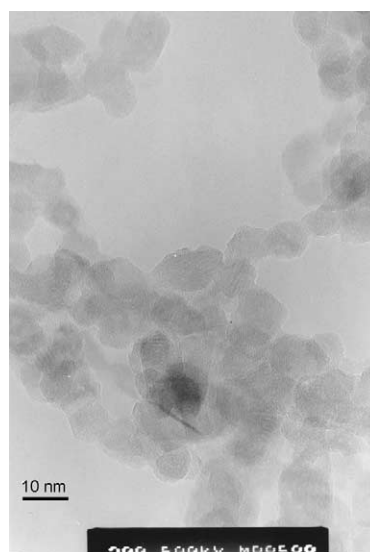


Fig. 5. TEM micrograph showing reticular planes of anatase nanocrystals displayed in Fig. 4.

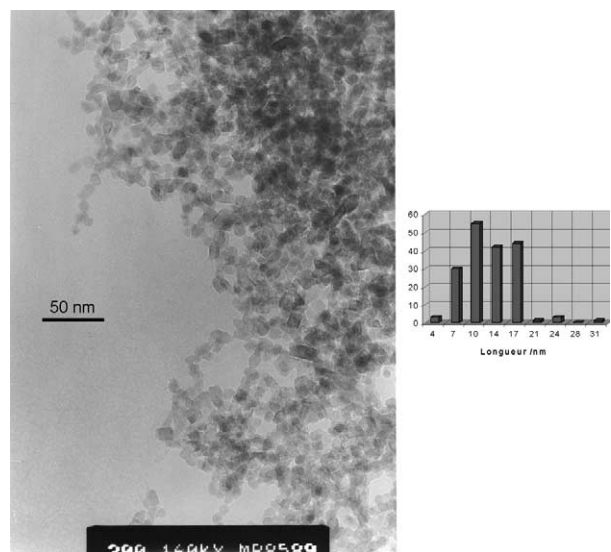


Fig. 4. TEM micrograph and size distribution of anatase nanocrystals obtained after hydrolysis and autoclaving ( $T = 200\text{ }^{\circ}\text{C}$ ) of  $\text{Ti}_6\text{O}_6(\text{OPr}^i)_6(\text{O}_2\text{CCH}_2\text{Ph})_6$  solutions at  $R = \text{Ti}/\text{NMe}_4^+ = 3$ . Average sizes and standard deviations are  $12(4) \times 8(2)$  nm.

poxyde and it was hoped that the use of a much more stable oxo-carboxylate precursor would lead to better results. Figs 4 and 5 show the spectacular decrease in size [ $L = 12(4)$  nm and  $W = 8(2)$  nm] observed under exactly the same experimental conditions but with  $\text{Ti}(\text{OPr}^i)_4$  replaced by  $[\text{TiO}(\text{OPr}^i)(\text{PAA})]_6$ . Moreover, for a given  $R$  ratio ( $R = 3$ ), the anisotropic shape factor  $A = L/W$  of the nanocrystals is found to decrease slightly by replacing  $\text{Ti}(\text{OPr}^i)_4$  ( $A = 1.7$ ) by  $[\text{TiO}(\text{OPr}^i)$

$(\text{PAA})]_6$  ( $A = 1.5$ ). As  $[\text{TiO}(\text{OPr}^i)(\text{PAA})]_6$  displays a much more anisotropic molecular structure than  $\text{Ti}(\text{O-Pr}^i)_4$ , we conclude that under such rather drastic conditions (base hydrolysis), the molecular information is lost during nucleation and growth of the anatase nanocrystals. Nevertheless, Fig. 4 shows that PAA ligands still play a major role concerning the size of the particles and their size distribution, which appears to be much more regular. For  $R = \text{Ti}/\text{Me}_4\text{N}^+ = 1$ , we found that the size of the particles have doubled in both directions [ $L = 29(10)$  nm and  $W = 16(4)$  nm] (Fig. 6) and that a bimodal size distribution was obtained. These results are in deep contrast with those obtained with  $\text{Ti}(\text{OPr}^i)_4$ , where decreasing the  $R$  ratio led to a considerable elongation of the anatase nanocrystals. For  $R = \text{Ti}/\text{Me}_4\text{N}^+ = 0.5$  (Fig. 7), we get a very broad size distribution characterised by  $L = 31(12)$  nm and  $W = 17(5)$  nm, instead of a regular array of hexagonal shaped nanocrystals with 13.5 nm diameter [3]. It is then obvious that the nucleation/growth steps are considerably perturbed by the presence of the PAA ligands. A possible explanation would be that, owing to their negative charge, phenylacetate  $\text{PhCH}_2\text{COO}^-$  ions are able to form ion-pairs with  $\text{NMe}_4^+$  cations preventing their specific adsorption on the [101] faces of the anatase nanocrystals. As this adsorption was invoked to explain the particular morphology of  $\text{Ti}(\text{OPr}^i)_4$ -derived nanoparticles [3], ion pairing in solution is expected to have a deep effect on morphologies and/or sizes. In our case, the global increase in size and polydispersity observed as  $R$  decreases should then be the simple consequence of a higher solubility of  $\text{TiO}_2$  with increasing base concentration.

In conclusion to this preliminary study, we think to have demonstrated that steric and acido-basic consid

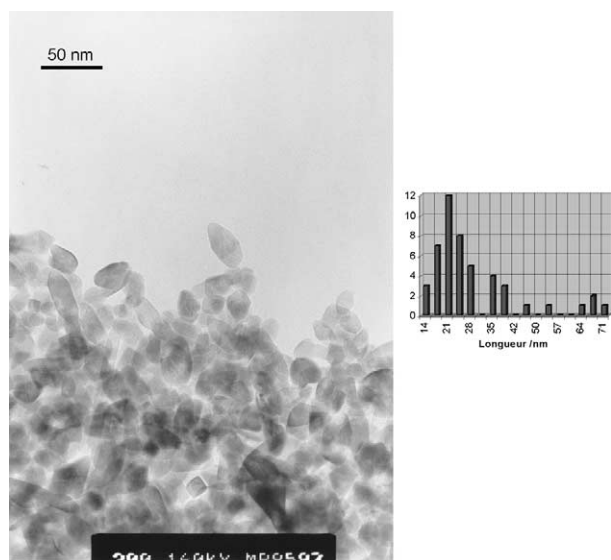


Fig. 6. TEM micrograph and size distribution of anatase nanocrystals obtained after hydrolysis and autoclaving ( $T = 200\text{ }^{\circ}\text{C}$ ) of  $\text{Ti}_6\text{O}_6(\text{OPr}^i)_6(\text{O}_2\text{CCH}_2\text{Ph})_6$  solutions at  $R = \text{Ti}/\text{NMe}_4^+ = 1$ . Average sizes and standard deviations are  $29(10) \times 16(4)$  nm.

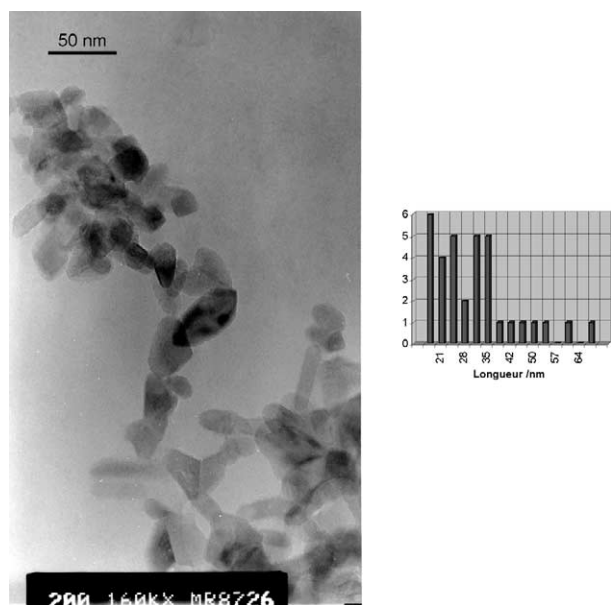


Fig. 7. TEM micrograph and size distribution of anatase nanocrystals obtained after hydrolysis and autoclaving ( $T = 200\text{ }^{\circ}\text{C}$ ) of  $\text{Ti}_6\text{O}_6(\text{OPr}^i)_6(\text{O}_2\text{CCH}_2\text{Ph})_6$  solutions at  $R = \text{Ti}/\text{NMe}_4^+ = 0.5$ . Average sizes and standard deviations are  $31(12) \times 17(5)$  nm.

erations alone are not sufficient to explain the various molecular shapes displayed by currently known oxo-carboxylate complexes. It then seems that without a full and detailed kinetic study of these systems, the basic mechanisms leading to the formation of these oxo compounds cannot be evidenced and understood. Obviously, despite the presence of oxo groups, considerable structural rearrangements can still occur in

solution and these systems cannot be qualified as being rigid and/or inert as other polynuclear carboxylate complexes. Consequently, it is our feeling that the very high lability of these compounds may be the key to understanding the apparent lack of shape selectivity. If kinetic effects are indeed important, the role of the solvent should also have to be studied in more details. We have also shown that nucleation and growth of nanocrystalline materials was deeply affected by the underlying molecular chemistry of the starting precursors. Consequently, if altering the size and shape of anatase nanocrystals is possible by playing with the  $R = \text{Ti}/\text{Me}_4\text{N}^+$  ratio, it may also not be very reproducible. Without reproducible results, it is then hard to speak of a good control of the nucleation and growth processes; considerable work remains to be done before achieving this goal. Moreover, we are still not in position to say if this control will be better through chemistry (as tried in this work) or through a very sharp tuning of all pertinent physico-chemical factors (a more conventional approach used in reference [3]). Nevertheless, we hope that this work will stimulate more intensive research in the fields of titanium oxo-carboxylate coordination chemistry and of titania solid-state nanochemistry.

### 3. Experimental section

All reagents were commercial products purchased from Aldrich in the highest purity available and were used without further purification. The starting  $\text{NMe}_4\text{OH}$  solution was 25 wt% in water, i.e.  $2.76\text{ mol}\cdot\text{l}^{-1}$ .  $^1\text{H}$  and  $^{13}\text{C}$  NMR spectra were recorded at 200 MHz on a Bruker WP200 SY spectrometer. FT-IR spectra were recorded between  $400\text{--}4000\text{ cm}^{-1}$  on a Bruker IF25 spectrometer. For TEM measurements, suspensions were allowed to dry on to a holey carbon film, which has previously been deposited on a copper grid. Observations were performed on a Topcon 002B microscope operating at a 200 kV accelerating voltage. The available point-to-point resolution was  $1.9\text{ \AA}$ . The presence of titanium in the observed nanoparticles has been checked by EDX spectroscopy since the microscope is equipped with a Si/Li detector allowing the performing of qualitative analysis. The occurrence of the anatase polymorph in the synthesised nanocrystals was also checked by TEM from their characteristic ring diffraction patterns. X-ray single crystal diffraction measurements have been made using an Enraf-Nonius diffractometer with graphite monochromated  $\text{Mo K}\alpha$  radiation. Further experimental details concerning crystal data (recording conditions, tables of atomic coordinates, anisotropic displacement parameters  $U_{ij}$ , bond distances and bond angles) are provided as supplementary materials. This

material has been deposited with the Cambridge Crystallographic Data Centre. Copies of the data can be obtained free of charge on application to CCDC, 12 Union Road, Cambridge CB2 1EZ, UK [fax int. code + 44(0)1223/336-033, e-mail: deposit@ccdc.cam.ac.uk] quoting the depository number CCDC-165152.

### 3.1. Spectroscopic data of reagents

Phenylacetic acid: IR (neat)  $\nu$  (cm<sup>-1</sup>) 3 200–2 500s ( $\nu$  O–H,  $\nu$  C–H), 1 708s ( $\nu$  C–O), 1 243s, 925s; <sup>1</sup>H NMR (CDCl<sub>3</sub>)  $\delta$  3.66 (s, 2H, –CH<sub>2</sub>COOH), 7.33 (m, 5H, C<sub>6</sub>H<sub>5</sub>–), 10.9 (s, 1H, –COOH); <sup>13</sup>C NMR (CDCl<sub>3</sub>)  $\delta$  41.23 (–CH<sub>2</sub>COOH), 127.48, 128.79, 129.51, 133.41 (C<sub>6</sub>H<sub>5</sub>–), 178.16 (–COOH)

Ti(OPr<sup>*i*</sup>)<sub>4</sub>: <sup>1</sup>H NMR (CD<sub>2</sub>Cl<sub>2</sub>)  $\delta$  1.24 (d, *J* 6.1 Hz, 6H, CH<sub>3</sub>), 4.48 (sept, *J* 6.1 Hz, 1H, CH); <sup>13</sup>C NMR (CD<sub>2</sub>Cl<sub>2</sub>)  $\delta$  26.47 (CH<sub>3</sub>), 75.94 (OCH); <sup>17</sup>O NMR (CD<sub>2</sub>Cl<sub>2</sub>)  $\delta$  293 (OCH(CH<sub>3</sub>)<sub>2</sub>).

### 3.2. Preparation of Ti<sub>6</sub>(μ<sub>3</sub>-O)<sub>6</sub>(C<sub>6</sub>H<sub>5</sub>CH<sub>2</sub>COO)<sub>6</sub>(OPr<sup>*i*</sup>)<sub>6</sub> 1

Colourless prismatic crystals were formed within two weeks from a clear colourless solution obtained by injecting under vigorous stirring 5 ml of a solution containing 0.53 g (3.9 mmol) of phenylacetic acid in acetone into 5 mL of a solution containing 0.74 g (2.6 mmol) of titanium isopropoxide in 2-propanol.

### 3.3. X-ray structure analysis of 1

Ti<sub>6</sub>O<sub>24</sub>C<sub>66</sub>H<sub>84</sub>, *M* = 1 548.79 g mol<sup>-1</sup>, triclinic, space group *P* $\bar{1}$ , *a* = 1 037.58(4), *b* = 1 357.48(5), *c* = 1423.06(6) pm,  $\alpha$  = 104.245(5)°,  $\beta$  = 107.036(5)°,  $\gamma$  = 99.402(5)°, *U* = 1796.5(4)·10<sup>6</sup> pm<sup>3</sup>, *d*<sub>calcd</sub> = 1.43 g cm<sup>-3</sup> for *Z* = 1. *F* (000) = 804, graphite-monochromated Mo K $\alpha$  radiation,  $\mu$  = 0.710 mm<sup>-1</sup>,  $\lambda$  = 71.073 pm, *T* = 173 K, crystal size = 0.20 × 0.12 × 0.10 mm. Data were collected on a Nonius Kappa CCD diffractometer by a combination of five set of exposures (12 176 reflections measured and 8151 unique) in the range 2.5° ≤  $\theta$  ≤ 27.43°. The structure was solved using direct methods and refined against |*F*| [5714 reflections having *I* > 3  $\sigma$ (*I*)]. Hydrogen atoms were introduced as fixed contributors when a residual electronic density was observed near their expected positions. For all computations the Nonius OpenMoleN package was used. Refinement converged at *R*<sub>1</sub> = 0.038, *wR*<sub>2</sub> = 0.058 {*w* = 4 *F*<sub>0</sub><sup>2</sup>/[ $\sigma^2$ (*F*<sub>0</sub><sup>2</sup>) + 0.006 4 *F*<sub>0</sub><sup>4</sup>]}; final GOF = 1.008. The final difference map showed no peak larger than +0.544 e·Å<sup>-3</sup> and no hole larger than –0.122 e·Å<sup>-3</sup>.

### 3.4. Spectroscopic data for 1

IR (KBr)  $\nu$  (cm<sup>-1</sup>) 3420w ( $\nu$  O–H), 2900–3090s ( $\nu$  C–H), 1610s, 1544s, 1435s ( $\nu$  C–O), 1163m, 1128s, 1008s, 858m, 704s, 629s, 466 s, 386s ( $\nu$  Ti–O)

<sup>1</sup>H NMR (CDCl<sub>3</sub>):  $\delta$  1.19 (d, 36H, OCH(CH<sub>3</sub>)<sub>2</sub>), 3.46 (s, 12H, CH<sub>2</sub>COO), 4.85 (sept, 6H, OCH(CH<sub>3</sub>)<sub>2</sub>), 7.25 (m, 30H, C<sub>6</sub>H<sub>5</sub>)

<sup>13</sup>C NMR (CDCl<sub>3</sub>):  $\delta$  24.4 [OCH(CH<sub>3</sub>)<sub>2</sub>], 42.6 (CH<sub>2</sub>COO), 81.9 [TiOCH(CH<sub>3</sub>)<sub>2</sub>], 126.3 (C<sub>6</sub>H<sub>5</sub> para), 128.0 (C<sub>6</sub>H<sub>5</sub> meta), 129.4 (C<sub>6</sub>H<sub>5</sub> ortho), 135.5 (OOCCH<sub>2</sub>C<sub>6</sub>H<sub>5</sub>), 177.3 (CH<sub>2</sub>COO).

### 3.5. Hydrolysis of Ti(OPr<sup>*i*</sup>)<sub>4</sub> at R = Ti/NMe<sub>4</sub><sup>+</sup> = 3

An aqueous solution of NMe<sub>4</sub>OH (0.04 ml in 150 ml of water = 0.11 mmol) is introduced into a three-necked flask having side necksfitted with a thermometer and a gas inlet tube (nitrogen gas). After cooling this solution down to 2 °C, a solution of 0.1 g (0.3 mmol) of titanium isopropoxide into 2-propanol (10 ml) is added dropwise under vigorous magnetic stirring. During the course of addition, a white precipitate is first formed, which undergoes partial redissolution upon stirring. After the addition was complete, the ice bath was replaced by an oil bath and the mixture heated under reflux (*T* ~ 90 °C) overnight. During the first hours, the solution was clear and became progressively more turbid during the last hours. This turbid solution was then transferred into a 120 mL stainless steel teflon-lined autoclave and again heated at 200 °C overnight.

### 3.6. Hydrolysis of [TiO(OPr<sup>*i*</sup>)(PAA)]<sub>6</sub> at R = Ti/NMe<sub>4</sub><sup>+</sup> = 3

The same experiment as above was repeated with an aqueous solution of NMe<sub>4</sub>OH (0.023 mL in 150 ml of water = 0.064 mmol) and 0.05 g (0.19 mmol) of [TiO(OPr<sup>*i*</sup>)(PAA)]<sub>6</sub> in THF (10 ml). After refluxing this solution overnight, the resulting turbid solution was autoclaved for one night at 200 °C.

### 3.7. Hydrolysis of [TiO(OPr<sup>*i*</sup>)(PAA)]<sub>6</sub> at R = Ti/NMe<sub>4</sub><sup>+</sup> = 1

The same experiment as above was repeated with an aqueous solution of NMe<sub>4</sub>OH (0.15 ml in 150 ml of water = 0.41 mmol) and 0.11 g (0.43 mmol) of [TiO(OPr<sup>*i*</sup>)(PAA)]<sub>6</sub> in THF (10 ml). After refluxing this solution overnight, the resulting turbid solution was autoclaved for one night at 200 °C.

### 3.8. Hydrolysis of [TiO(OPr<sup>*i*</sup>)(PAA)]<sub>6</sub> at R = Ti/NMe<sub>4</sub><sup>+</sup> = 0.5

The same experiment as above was repeated with an aqueous solution of NMe<sub>4</sub>OH (0.44 mL in 150 mL of water = 1.21 mmol) and 0.16 g (0.62 mmol) of [TiO(OPr<sup>*i*</sup>)(PAA)]<sub>6</sub> in THF (10 mL). After refluxing this solution overnight, the resulting turbid solution was autoclaved for one night at 200 °C.

**Acknowledgements.** The authors are indebted to A. De Cian, J. Fischer, and N. Gruber-Kyritsakas for recording crystal data and crystal structure determination. We are also indebted to M. Richard for technical assistance in obtaining TEM images.

## References

- [1] Elder S.H., Cot F.M., Su Y., Heald S.M., Tyryshkin A.M., Bowman M.K., Gao Y., Joly A.G., Balmer M.L., Kolwaite A.C., Magrini K.A., Blake D.M., *J. Am. Chem. Soc.* 122 (2000) 5138.
- [2] Rabenau A., *Angew. Chem. Int. Ed. Engl.* 24 (1985) 1026.
- [3] Chemseddine A., Moritz T., *Eur. J. Inorg. Chem.* 235 (1999).
- [4] Gautier-Luneau I., Mosset A., Galy J., *Z. Krist.* 180 (1987) 83.
- [5] Dœuff S., Dromzee Y., Taulelle F., Sanchez C., *Inorg. Chem.* 28 (1989) 4439.
- [6] Dœuff S., Dromzee Y., Sanchez C., *C. R. Acad. Sci. Paris, série II* 308 (1989) 1409.
- [7] Laaziz I., Larbot A., Guizard C., Durand J., Cot L., Joffre J., *Acta C., Acta Crystallogr.* C46 (1990) 2332.
- [8] Schubert U., Tewinkel S., Möller F., *Inorg. Chem.* 34 (1995) 995.
- [9] Barrow H., Brown D.A., Alcock N.W., Clase H.J., Wallbridge M.G.H., *J. Chem. Soc. Chem. Commun.* (1995) 1231.
- [10] Lei X., Shang M., Fehler T.P., *Organometallics* 15 (1996) 3779.
- [11] Lei X., Shang M., Fehler T.P., *Organometallics* 16 (1997) 5289.
- [12] Boyle T.J., Alam T.M., Tafoya C.J., Scott B.L., *Inorg. Chem.* 37 (1998) 5588.
- [13] Kickelbick G., Schubert U., *Eur. J. Inorg. Chem.* (1998) 159.
- [14] Papiernik R., Hubert-Pfalzgraf L.G., Vaissermann J., Goncalves M.C.H.B., *J. Chem. Soc. Dalton Trans.* (1998) 2285.
- [15] Pandey A., Gupta V.D., Nöth H., *Eur. J. Inorg. Chem.* (2000) 1351.
- [16] Sanchez C., Livage J., Henry M., Babonneau F., *J. Non-Cryst. Solids* 100 (1988) 65.
- [17] Eddaoudi M., Moler D.B., Li H., Chen B., Reineke T.M., O'Keefe M., Yaghi O.M., *Acc. Chem. Res.* 34 (2001) 319.
- [18] Campana C.F., Chen Y., Day V.W., Klemperer W.G., Sparks R.A., *J. Chem. Soc. Dalton Trans.* (1996) 691.
- [19] Day V.W., Eberspacher T.A., Klemperer W.G., Park C.W., *J. Am. Chem. Soc.* 115 (1993) 8469.
- [20] Pajot N., Papiernik R., Hubert-Pfalzgraf L.G., Vaissermann J., Parraud S., *J. Chem. Soc. Chem. Commun.* (1995) 1817.
- [21] Lide D.R. (Ed.), *Handbook of Chemistry and Physics*, 81st ed, CRC Press, 2000, pp. 8–46.
- [22] Cen W., Haller K.J., Fehlner T.P., *Inorg. Chem.* 32 (1993) 995.